Two-Dimensional Diffusion-Ordered NMR Spectroscopy as a Tool for Monitoring Functionalized Carbon Nanotube Purification and Composition

Riccardo Marega,[†] Vincent Aroulmoji,[‡] Massimo Bergamin,[‡,§] Luigi Feruglio,[†] Francesca Dinon,[§] Alberto Bianco,[⊥] Erminio Murano,[‡,§,*] and Maurizio Prato[†,*]

[†]Center of Excellence for Nanostructured Materials (CENMAT), Dipartimento di Scienze Farmaceutiche and INSTM UdR Trieste, Università degli Studi di Trieste, Piazzale Europa 1, 34127 Trieste, Italy, [‡]Protos Research Institute, Via Flavia 23/1, c/o Sviluppo Italia, 34148, Trieste, Italy, [§]Polymer Conjugation Department, EURAND S.p.A, Area Science Park, Padriciano 99, 34149 Trieste, Italy, and [⊥]CNRS, Institut de Biologie Moléculaire et Cellulaire, Laboratoire d'Immunologie et Chimie Thérapeutiques, 67000 Strasbourg, France

ABSTRACT Functionalized carbon nanotube (CNT) derivatives are currently under thorough investigation in different biomedical investigations. In this field of research, the composition of sample either in terms of covalently attached or physisorbed moieties can greatly affect the observed results and hamper the comparison between different studies. Therefore, the availability of a fast and reliable analytical technique to assess both the type of interaction (covalent *vs* noncovalent) and the composition of CNT conjugates is of great importance. Here we describe that the two-dimensional diffusion-ordered (DOSY) NMR spectroscopy is extremely useful to discriminate between conjugated and unconjugated polyethylene glycol groups in samples obtained by condensation with oxidized single-walled carbon nanotubes (SWNTs). This fast and nondestructive technique allows us to follow the removal of unconjugated polyethylene glycol chains during the purification. In particular, DOSY analysis reveal that about $^1/_3$ (wt %) of the polyethylene glycol used for the condensation remained physisorbed to functionalized SWNTs after dialysis. Complete elimination of physisorbed polyethylene glycol was achieved using diafiltration.

KEYWORDS: carbon nanotube · covalent functionalization · DOSY · NMR · purification

Carbon nanotubes (CNTs), either single-walled (SWNTs)[1] or multi-walled (MWNTs),[2] are under thorough investigation for their potential applications in several biomedical[3−6] and nanotechnological fields.[7−9] A wide number of derivatization protocols have been proposed and evaluated to modify commercially available CNT samples, in order to decrease impurity content and modify length and diameter distribution as well as solubility/dispersibility in most common solvents.[10−12]

A common approach used to increase bioavailability of CNTs for biological assays is the covalent[13−17] and noncovalent[18,19] functionalization with polyethylene glycol (PEG) derivatives with different molecular weight (M_w).[20] Sun and co-workers investigated the conjugation chemistry between the carboxylic groups of oxidized-SWNTs (ox-SWNTs) and diamine-terminated polyethylene glycol. In particular, the acylation−amidation, the carbodiimide-mediated activation, and the ionic interactions were reported.[13,14] Sample purification was achieved by means of dialysis and centrifugation cycles, whereas the characterization of the products was based on solution ^{1}H or ^{13}C NMR spectroscopy,[21] thermogravimetric analysis (TGA), and various spectroscopic (UV−vis, NIR, FT-IR, Raman) and microscopy-based techniques (SEM and TEM). In the case of noncovalent pegylation approaches, several results suggest a strong interaction between PEG derivatives and SWNTs, also at relatively high temperatures.[18,19] Some pegylated CNT derivatives have potential applications in materials science,[22] but most of the studies regarding pegylated CNTs focus on understanding their biological behavior.[23−26] It is well-known that pegylation of nanostructures prevents nonspecific protein binding and may impart stealth properties and thus longer half-life during *in vivo* biodistribution studies.[27] Thus, since carbon nanostructures are under investigation as promising drug-delivery systems[4] and biomedical devices,[28−31] it is of great interest to understand how to follow and determine water-soluble CNT purification and composition, to easily evaluate and compare the biological responses after their administration. Since size-related purification procedures

*Address correspondence to prato@units.it, murano@protos-institute.org.

Received for review February 7, 2010 and accepted March 17, 2010.

Published online April 1, 2010.
10.1021/nn100257h

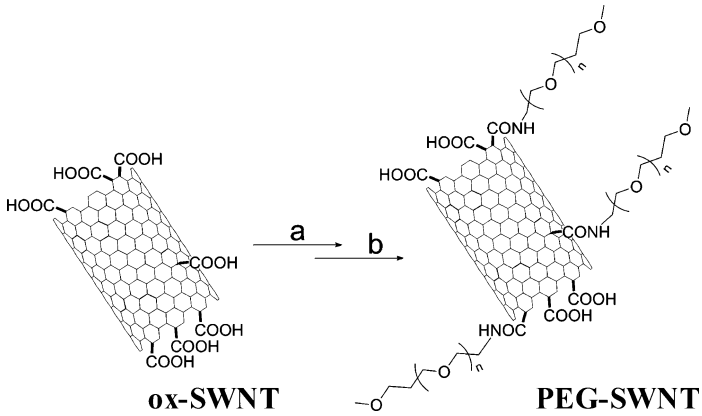

Scheme 1. Synthetic route to ox-SWNT pegylation: a = EDC · HCl, NHS, and DMAP in DMF, b = α-amino-ω-methoxy-polyethylene glycol ($M_w \approx$ 2000 g · mol^{-1}, n = 45) and DMAP in DMF.

are employed to purify and isolate pegylated CNTs, size-related analytical techniques could be used to achieve this objective. Two-dimensional diffusion-ordered NMR spectroscopy (2D-DOSY)[32] is rapidly emerging as a powerful analytical technique able to merge size-analysis with spectroscopic (chemical) characterization. It was applied for the evaluation of mixture composition (the so-called chromatography on a tube),[33] the low molecular-weight impurity detection,[34] the supramolecular assembly characterization,[35−39] the molecular-weight distribution assessment,[40,41] and the confirmation of macromolecule functionalization.[42] In the last years, chemically modified nanostructured materials, like nanoparticles,[43−46] dendrons,[38,47] and fullerenes[48,49] were also analyzed with this technique.

In a previous work, we took advantage of the different diffusive behavior of small organic amines and their ox-SWNT conjugates to assess the chemical interaction between these species,[50] by recording DOSY spectra at fixed, strong field gradients (1D-DOSY).[51] In that case, the weakness of the signals of the organic fraction, due to the low degree of functionalization, and the limited solubility in organic solvents, did not allow us to perform the 2D-DOSY analysis. On the other hand, pegylated SWNTs show reasonable water solubility, high amount of organic moiety and strong, characteristic signals in the ^{1}H NMR spectra, properties that well match with the requirements for a reliable and fast 2D-DOSY analysis.

Here we report the use of 2D-DOSY analysis of pegylated ox-SWNTs (PEG-SWNTs) to assess the degree of interaction between the starting components and to qualitatively monitor the conjugate composition. **PEG-SWNTs** were purified by dialysis and then by diafiltration, a more efficient purification technique. Each conjugate composition was analyzed by means of DOSY analysis. ^{1}H-relaxation time determination was used to control the T_1 relaxation time of the PEG chains after ox-SWNT conjugation, and compared with the DOSY findings. To the best of our knowledge, this report is the first attempt to monitor a water-soluble CNT derivative purification and composition by DOSY NMR analysis.

RESULTS AND DISCUSSION

HiPco pristine SWNTs were oxidized according to a two-step process previously described,[50,52] yielding carboxylated SWNTs (ox-SWNTs) with a short average length (180 ± 160 nm, by STM analysis)[52] and increased average diameter (0.9 nm by STM analysis and Raman spectroscopy) in comparison to pristine tubes.[52] The carboxylic groups of ox-SWNTs were first converted into *N*-hydroxysuccinimidyl (NHS) esters, as previously reported,[50] and then allowed to react with α-amino-ω-methoxy-polyethylene glycol (mPEG-NH$_2$, $M_w \approx$ 2000 g · mol^{-1}, Scheme 1).

After 72 h of stirring at room temperature, the reaction mixture was poured into deionized water, and subjected to centrifugation cycles at 5000 rpm, giving a black aqueous solution (see Experimental Section). The water-soluble fraction was dialyzed against deionized water using a cellulose membrane with a molecular weight cutoff of 12 000 g · mol^{-1} for 4 days, and freeze-dried to obtain **PEG-SWNT-a**. Figure 1 reports the signal intensity decays of the organic molecules present in the dialysis solution (Figure 1a) and the dialyzed fraction (Figure 1b), respectively, after 48 h of dialysis, as a function of the increasing field gradient strength. Such signal attenuation is a function of several parameters, including the original signal intensity (concentration) and the diffusion coefficient of the molecule, according to the Stejskal and Tanner equation.[53]

By least-squares fitting of these decay plots, it is possible to calculate the diffusion coefficient of each proton signal. The data can be presented in a 2D contour-mode plot where cross-peaks between the diffusion constant values and the chemical shifts are reported for each proton signal. Both the excess of reagents and the solvent were found in the dialysis solution (Figure 1a), since cross peaks of mPEG-NH$_2$ ($D = 1.52 \times 10^{-10}$ m^2 · s^{-1}, 3.59 ppm), DMAP ($D = 6.46 \times 10^{-10}$ m^2 · s^{-1}, 2.53, 6.63, and 7.93 ppm), EDC · HCl ($D = 6.46 \times 10^{-10}$ m^2 · s^{-1}, 0.95, 1.61, 2.33, 2.55 ppm), NHS ($D = 6.90 \times 10^{-10}$ m^2 · s^{-1}, 2.95 ppm), and DMF ($D = 9.00 \times 10^{-10}$ m^2 · s^{-1}, 2.90, 2.74, and 7.81 ppm) were clearly present in the 2D-DOSY plot. In the dialyzed fraction, instead, just cross peaks with shift values typical of the mPEG-NH$_2$ chains were detected, but with two different values in the diffusion domain ($D = 0.48 \times 10^{-10}$ m^2 · s^{-1}, 3.71 ppm and $D = 1.29 \times 10^{-10}$ m^2 · s^{-1}, 3.60 ppm, Figure 1d). After the third day of dialysis, only a cross peak related to mPEG-NH$_2$ chains was detected in the 2D-DOSY plot of the dialysis solution ($D = 1.42 \times 10^{-10}$ m^2 · s^{-1}, 3.60 ppm), while no cross-peaks due to residual solvent or excess reagents were detected (Supporting Information, Figure S1).

A portion of **PEG-SWNT-a** was isolated by freeze-drying, while the other was subjected to discontinuos

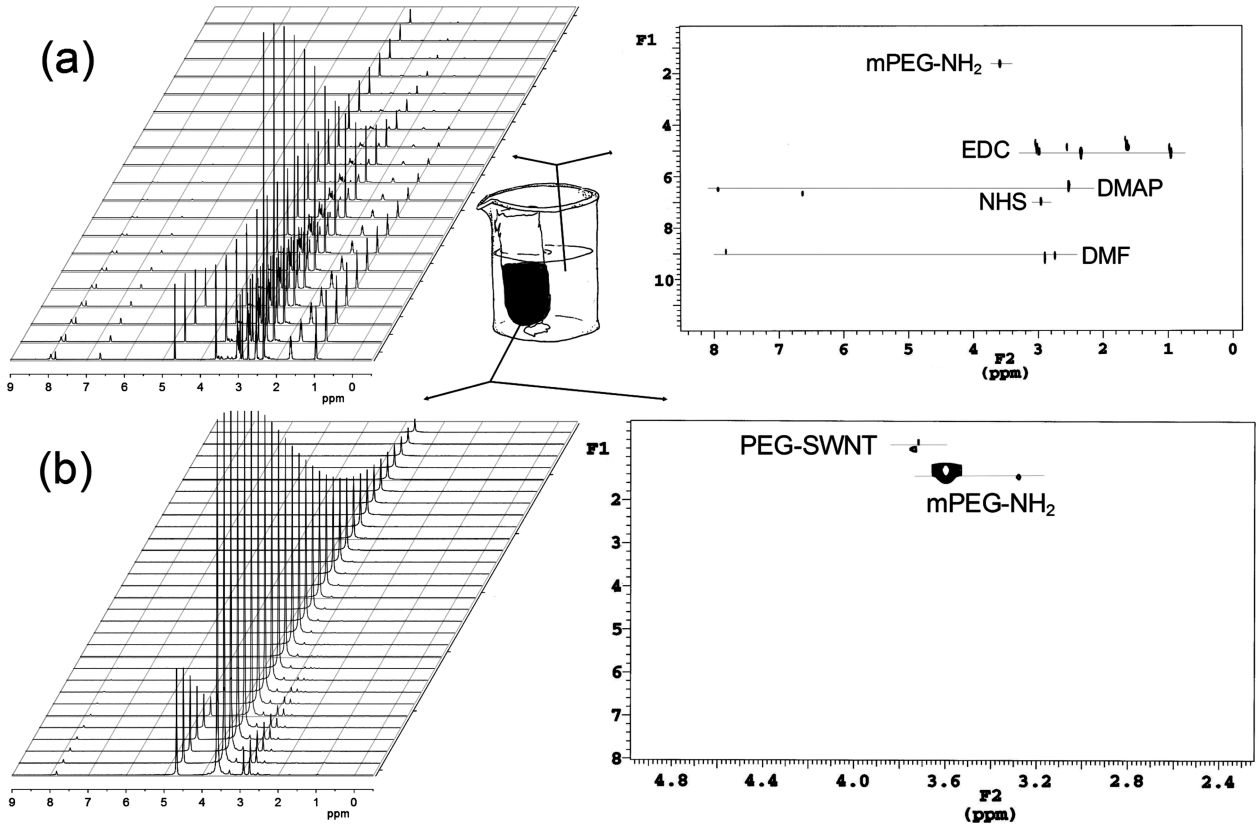

Figure 1. Signal intensity decay obtained with the 2D-DOSY analysis of the dialysis solution (a) and the dialyzed fraction (b) during PEG-SWNT-a isolation (second day). 2D-DOSY contour mode plots, where the shift-resolved discrimination of the diffusion constant can be visualized, are reported for the same fractions (top and bottom right, F_1 axis = $m^2 \cdot s^{-1} \times 10^{-10}$).

diafiltration. Diafiltration is a membrane-based purification technique commonly used for biological[54,55] and colloidal applications.[56] It is based on the different solute permeability with respect to a (nano)pore-sized membrane, thus this technique has also been used recently for other nanosized materials purification[11] and fractionation.[57,58]

Discontinuous diafiltration in suitable centrifugal concentrators takes advantage of centrifugation to force the membrane-based separation of the solutes, according to the different hydrodynamic radius. The diafiltered product was then freeze-dried, giving the fraction **PEG-SWNT-b** (Scheme 2).

Both **PEG-SWNT** fractions were preliminarily evaluated by TGA analysis in order to obtain an estimate of the $mPEG\text{-}NH_2$ amounts (Figure 2). The $mPEG\text{-}NH_2$ thermal behavior (Figure 2b) is characterized by a pyrolysis step in the range 200−480 °C, with a main, sharp decomposition between 300−450 °C, after that the polymer is completely decomposed (residual weight at 600 °C ~0%). On the basis of the observations made for $mPEG\text{-}NH_2$, the residual weight after 500 °C of **PEG-SWNT-a** (31.8% at 545 °C) can therefore be used to estimate the ox-SWNT content: assuming $mPEG\text{-}NH_2$ as a monodispersed molecule with $M_w \approx 2000$ g · mol^{-1}, a pegylation degree in the range ~0.3 μmol · mg^{-1}, and a SWNT content of about 32 wt % can be estimated for **PEG-SWNT-a**,[59] in agreement with the results reported by other groups (Figure 2c).[14,17,60] For **PEG-**

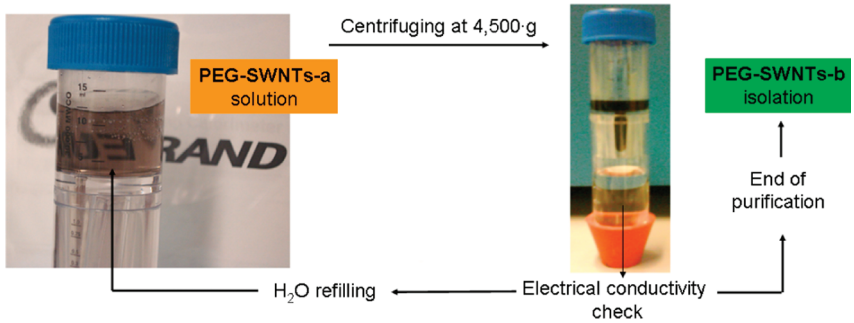

Scheme 2. PEG-SWNT-b isolation procedure by means of discontinuous diafiltration.

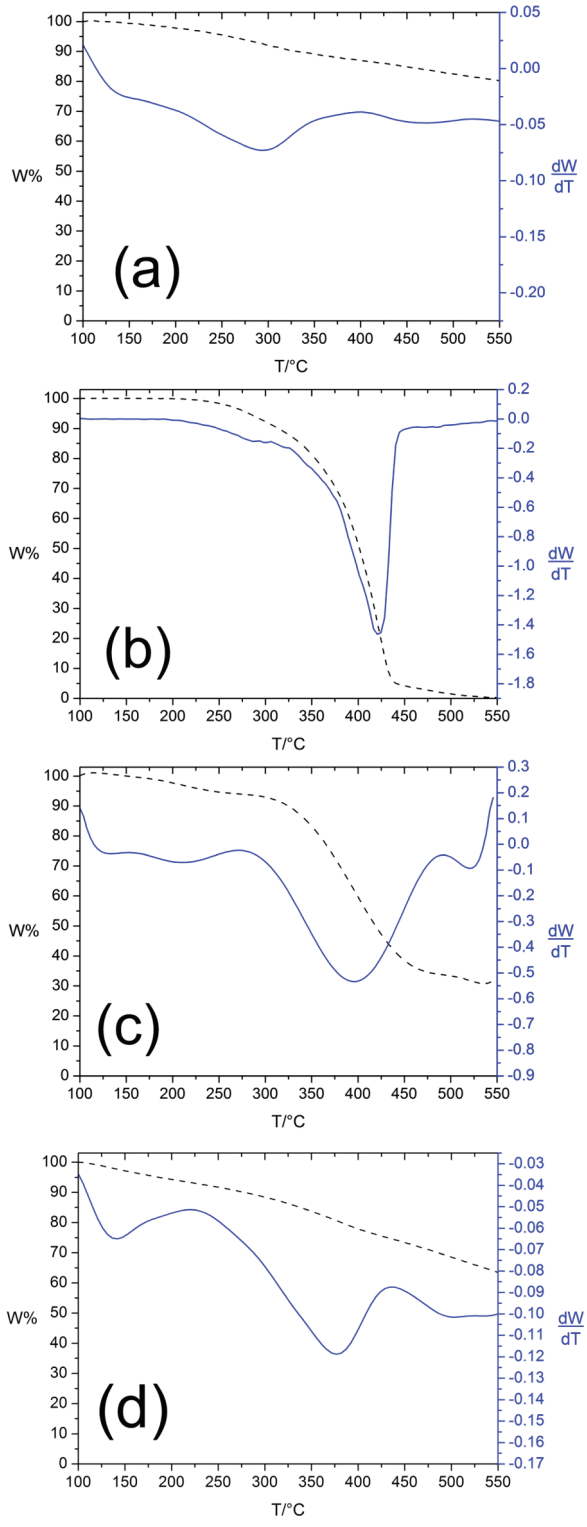

Figure 2. Temperature-modulated plots (---) and differential thermal plots (blue line) of (a) ox-SWNTs (4.180 mg), (b) mPEG-NH_2 (3.754 mg), (c) PEG-SWNT-a (0.644 mg), and (d) PEG-SWNT-b (0.562 mg) recorded under N_2 flow (20 mL · min^{-1}) and a temperature increase of 5 °C · min^{-1}.

SWNT-b the corresponding values are ~0.2 μmol · mg^{-1} and 64 wt %, respectively (Figure 2d).

To verify if these compositional results are reliable, a physical mixture with known amounts of mPEG-NH_2 (66 wt %) and ox-SWNTs (34 wt %) was prepared and characterized by TGA (Supporting Information, Figure S2). A narrow-range decomposition occurring between 300 and 475 °C, similar to that of pure mPEG-NH_2, and a residual weight (30.7% at 543 °C) very close to that of **PEG-SWNT-a** was obtained, suggesting the accuracy of the TGA-based estimate of the **PEG-SWNT-a** composition.

This set of data indicates that after the diafiltration step, the PEG moiety content in **PEG-SWNT-b** strongly decreased (~33 wt %). A summary of the TGA results is reported in Supporting Information, Table S3.

^{1}H NMR analysis of both **PEG-SWNT** fractions and mPEG-NH_2 was then performed (Figure 3). The spectrum of **PEG-SWNT-a** in D_2O solution shows a broad peak centered at 3.60 ppm, which is related to the polyethylene glycol moiety (Figure 3a). In this spectrum a shoulder can be observed at 3.50 ppm, previously described as part of a whole signal.[14,60] The proton spectrum of **PEG-SWNT-b** in D_2O solution is reported in Figure 2c. As a consequence of the diafiltration process (see Supporting Information, Figure S4), a strong reduction of the mPEG-NH_2 chain signal is observed, in agreement with the TGA findings. Furthermore, the shoulder at 3.50 ppm, even if not completely removed, shows a strong decrease in its intensity.

The peak broadening found in many proton spectra of CNT derivatives is connected with the altered proton-relaxation properties of the organic moieties after conjugation to CNTs. The reduced tumbling motions of the organic molecules once conjugated to such huge macromolecular structures, which exhibit different magnetic-field neighborhoods due to the "polydispersity" of their length, diameter, and conductivity, are mostly responsible for this effect.[13,61] To evaluate the peak broadening of the signal at 3.60 ppm found in the conjugate, longitudinal spin−lattice (T_1) relaxation time determination was carried out in D_2O solutions of both **PEG-SWNT-a** and mPEG-NH_2, using an inversion recovery pulse sequence (Supporting Information, Figure S5). The broad signal at 3.60 ppm of **PEG-SWNT-a** shows a T_1 value of 0.6000 ± 0,0045 s, while the sharp peak of mPEG-NH_2 has a value of 0.7600 ± 0,0028 s. The reduced relaxation time of **PEG-SWNT-a** protons ($\Delta \approx -21\%$) cannot be simply due to different shimming conditions, suggesting the altered proton-relaxation properties of these mPEG-NH_2 chains after ox-SWNT conjugation.[61] On the basis of these NMR findings, the diffusive behavior of the **PEG-SWNT** fractions was then evaluated by 2D-DOSY analysis. The signal attenuation as a function of the increasing field-gradient strength is reported in Figure 4.

The 2D-DOSY stacked-plot of **PEG-SWNT-a** clearly shows that, as the field-gradient strength increases, the absolute intensity of the peak at 3.50 ppm rapidly decreases. On the other hand, the absolute intensity of the dominant, broad signal at 3.60 ppm is less affected

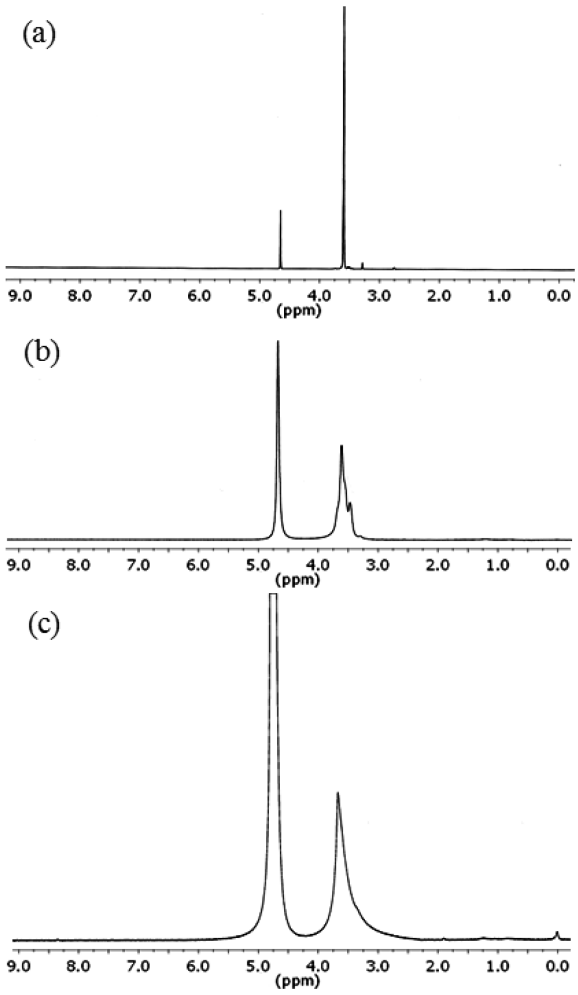

Figure 3. ^{1}H NMR spectra of D_2O solutions of mPEG-NH_2 (a), **PEG-SWNT-a** (b), and **PEG-SWNT-b** (c).

as the field-gradient strength increases. Since the signal intensity attenuation is strictly related to the diffusion coefficient of the spin-systems in solution,[53] the results in Figure 4a suggest that there are at least two differently diffusing mPEG-NH_2 moieties. The stronger signal attenuation is usually observed for the smaller, faster diffusing molecules, in this case the unconjugated mPEG-NH_2 chains. On the other hand, the small attenuation of the broad, faster relaxing signal at 3.60 ppm is connected with a strongly reduced diffusion of a mPEG-NH_2 moiety, which can be attributed to the conjugated fraction. The 2D-DOSY stacked plot of **PEG-SWNT-b** signals decay is reported in Figure 4b, which shows one broad signal at 3.61 and a strong attenuation of the small shoulder at 3.50 ppm. These findings suggest that the unconjugated mPEG-NH_2 moiety, if not completely removed, was at least strongly reduced after the further purification step.

To better visualize the differences in the PEG-SWNT composition during the purification steps, the exponential signal decays of both **PEG-SWNT** fractions were least-squares fitted, allowing the calculation of the diffusion coefficients. The 2D-DOSY contour-mode plots reporting the shift-resolved diffusion coefficient discrimination are displayed in Figure 5. It should be pointed out that the computation of the diffusion coefficients was carried out to qualitatively distinguish between the main components present in the PEG-SWNT D_2O solutions and therefore obtain a TLC-like characterization of their content during the purification steps.

In fact, in the **PEG-SWNT-a** plot (Figure 5a) the signals arising from water molecules ($D = 14.64 \times 10^{-10}$ $m^2 \cdot s^{-1}$, 4.66 ppm), the conjugated PEG moiety ($D = 0.60 \times 10^{-10}$ $m^2 \cdot s^{-1}$, 3.59 ppm) and the faster diffusing ($D = 3.37 \times 10^{-10}$ $m^2 \cdot s^{-1}$, 3.45 ppm) unconjugated mPEG-NH_2 chains were resolved.

The **PEG-SWNT-b** plot (Figure 5b), instead, shows only water molecules ($D = 17.34 \times 10^{-10}$ $m^2 \cdot s^{-1}$, 4.69 ppm) and the slower diffusing, conjugated PEG moiety ($D = 1.09 \times 10^{-10}$ $m^2 \cdot s^{-1}$, 3.61 ppm). Even if the **PEG-SWNT** solutions for the 2D-DOSY analysis were prepared with the same ox-SWNT equivalent content, the absence, or at least strong removal, of the mPEG-NH_2 portion determined higher diffusion coefficients for both water and PEG-SWNTs in the **PEG-SWNT-b** frac-

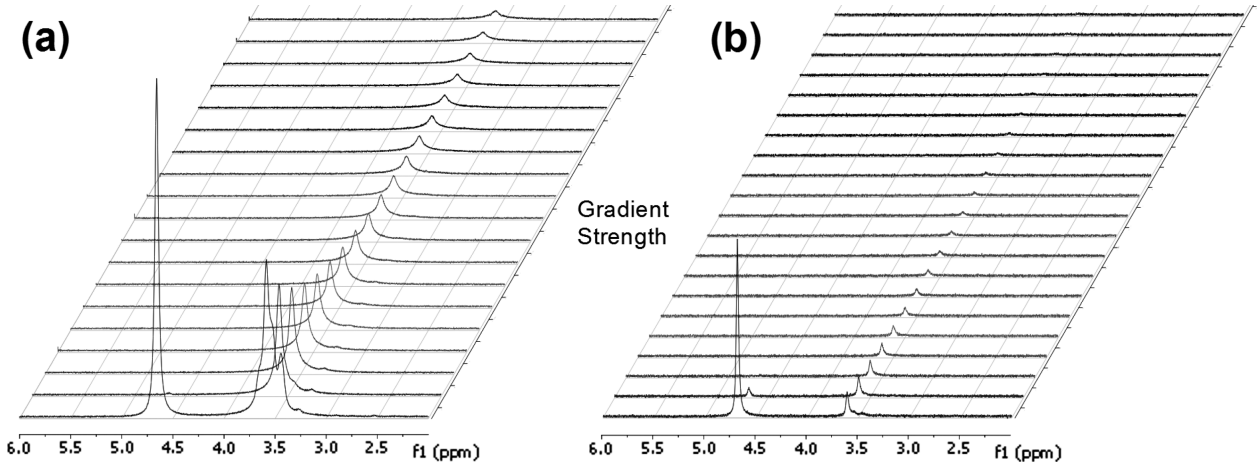

Figure 4. Stacked-plot of the signal intensity decay of PEG-SWNT-a (a) and PEG-SWNT-b (b) from 2D-DOSY analysis with increasing pulsed field-gradient strength (from 1.97 to 53.2 G · cm^{-1} in 20 steps).

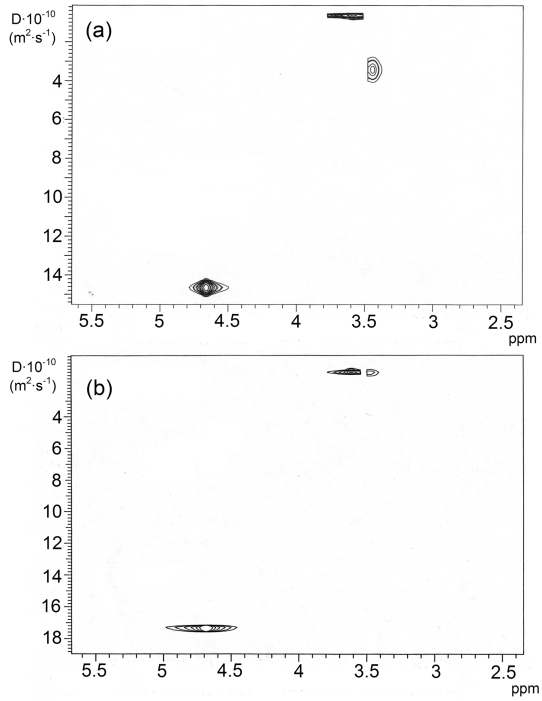

Figure 5. Contour-mode 2D-DOSY plots after least-squares fit of PEG-SWNT-a (a) and PEG-SWNT-b (b) in D_2O solutions.

tion. Several factors can contribute to such variation, like the possible small difference in the viscosity between the two deuterated solutions or the error associated with the TGA-based estimate of the fraction composition. But we have also to consider that the unconjugated mPEG-NH_2 chains in **PEG-SWNT-a** can interact with both PEG-SWNTs and water molecules in a dynamic and fast (on the NMR time scale) way: therefore an apparent reduction of both PEG-SWNT and water molecules diffusion behavior was observed by 2D-DOSY analysis.

A different mathematical approach for the signal decay data-treatment, based on the generalized iterative fixed-point algorithm (GIFA)[62] afforded the same discrimination in the diffusion domain ascertained after least-squares fitting (Supporting Information, Figure S6). We cannot exclude that traces of mPEG-NH_2 remained after the diafiltration procedure, but these diffusion-based results confirm the different diffusive behavior of conjugated and unconjugated mPEG-NH_2 fractions and the apparent removal of the unconjugated moiety after diafiltration, in agreement with the TGA findings.

CONCLUSIONS

After ox-SWNT pegylation, the degrees of interaction between the starting material and the conjugate composition have been assessed through diffusion-based NMR analysis and TGA evaluation. After the conjugate purification by dialysis, two different signals belonging to the same organic functionality were discriminated in the diffusion domain and then attributed to the conjugated and unconjugated PEG fractions. Longitudinal T_1 relaxation time determination suggests altered proton relaxation properties of the conjugated PEG chains, consistent with their reduced diffusion in solution. These findings are supported by the "chromatography-like" indications of the 2D-DOSY analysis and the TGA composition evaluation after the further **PEG-SWNT** purification through diafiltration. Preliminary studies suggest that also biopolymer conjugated ox-SWNTs and dendron-functionalized MWNTs[63] can be evaluated in water solutions by this promising analytical technique. Since many examples of polymer-functionalized, water-soluble CNT derivatives have been reported in recent years, we suggest 2D-DOSY analysis as a new quick and versatile tool for monitoring both conjugation and qualitative product composition of these important and promising nanosized derivatives.

EXPERIMENTAL SECTION

General. SWNTs produced by HiPco technique were purchased from Carbon Nanotechnologies, Inc. (lot no. R0510c) and oxidized by a two-step oxidative treatment as previously reported.[52] α-Amino-ω-methoxy-polyethylenglycol ($M_w \approx 2000$ g · mol^{-1}) was purchased from Sunbio Inc. (lot no. CIAM-002-04112). Cellulose dialysis tube (D9527-100FT, cutoff 12000 g · mol^{-1}) were purchased from Sigma-Aldrich, while centrifugal concentrators (Vivaspin R20, cutoff 10000 g · mol^{-1}) were obtained from Sartorius Stedim Biotech.

Pegylation of ox-SWNTs. ox-SWNTs (50.0 mg, 140 μmol of COOH) in DMF (15 mL) were sonicated in a water bath for 20 min to give a black homogeneous suspension. Then 4-dimethylaminopyridine (DMAP, 21.0 mg, 172.13 μmol) was added, and sonication continued for 10 min. *N*-Hydroxysuccinimide (NHS, 61.2 mg, 532.2 μmol) was added to ox-SWNT dispersion, and sonication continued for other 10 min. A solution of *N*-ethyl-*N*′-(3-dimethylaminopropyl)-carbodiimmide hydrochloride (EDC · HCl, 83.7 mg, 436.6 μmol) and DMAP (51.5 mg, 422.2 μmol) in DMF (5 mL) was slowly added to the ox-SWNT dispersion. The reaction mixture was sonicated for 1 h and then stirred for 2 h at room temperature. Then a solution of α-amino-ω-methoxy-polyethylenglycol ($M_w \approx 2000$ g · mol^{-1}, 300 mg) and DMAP (150 μmol) in 5 mL of DMF was added to the reaction mixture, which was then vigorously stirred at room temperature for 72 h, affording an homogeneous black dispersion.

Isolation of PEG-SWNT Fractions. The PEG-SWNT reaction mixture was poured in 80 mL of H_2O and centrifuged at 5000 rpm for 15 min, allowing collection of the soluble PEG-SWNT fraction. The black precipitates were combined in 100 mL of H_2O and sonicated for 15 min before being centrifuged at 4500 rpm for 15 min. By combining the supernatants, about 200 mL of a black solution were collected and put in a cellulose dialysis tube (cutoff 12 000 g · mol^{-1}) for dialysis against deionized H_2O (at least four replacements each day, four days for the overall dialysis). After dialysis, half of the purified solution was concentrated on a rotatory evaporator to 10−15 mL, before being sonicated for 15 min in a water bath and freeze-dried affording **PEG-SWNT-a**. The remaining portion of the dialyzed solution was poured in four centrifugal concentrators (20 mL tubes) and centrifuged at 4500 g for 15 min. Progressively the solution concentrated and

thus saturation occurred, therefore after each two centrifuging cycles the retentate compartment was withdrawn, poured in an Erlenmeyer flask, and sonicated for 5 min to help the dispersion homogenization. When only 20 mL of saturated solution was obtained, about 4−6 centrifuging cycles with subsequent deionized H_2O additions were performed to observe a strong decrease of the filtrate conductivity, until it matched that of deionized H_2O. Finally, the saturated solution in the retentate (about 10−15 mL) was freeze-dried, allowing the isolation of the **PEG-SWNT-b** fraction.

Acknowledgment. This work was financially supported by the University of Trieste, INSTM, MIUR (PRIN 2008, prot. 20085M27SS and Firb, prot. RBNE033KMA), and the "Agence National de la Recherche" (ANR-05-JCJC-0031-01).

Supporting Information Available: Detailed experimental procedure, instrumental and software settings, full TGA data results, supporting diffusion-based and other conventional NMR results, TEM characterization of the D_2O solution content. This material is available free of charge *via* the Internet at http://pubs.acs.org.

REFERENCES AND NOTES

1. Iijima, S.; Ichihashi, T. Single-Shell Carbon Nanotubes of 1-nm Diameter. *Nature* **1993**, *363*, 603–605.
2. Iijima, S. Helical Microtubules of Graphitic Carbon. *Nature* **1991**, *354*, 56–58.
3. Kostarelos, K.; Bianco, A.; Prato, M. Promises, Facts, and Challenges for Carbon Nanotubes in Imaging and Therapeutics. *Nat. Nanotechnol.* **2009**, *4*, 627–633.
4. Prato, M.; Kostarelos, K.; Bianco, A. Functionalized Carbon Nanotubes in Drug Design and Discovery. *Acc. Chem. Res.* **2008**, *41*, 60–68.
5. Bianco, A.; Kostarelos, K.; Prato, M. Opportunities and Challenges of Carbon-Based Nanomaterials for Cancer Therapy. *Expt. Opin. Drug Deliv.* **2008**, *5*, 331–342.
6. Lu, F.; Gu, l.; Meziani, M. J.; Wang, X.; Luo, P. G.; Veca, L. M.; Cao, L.; Sun, Y. P. Advances in Bioapplications of Carbon Nanotubes. *Adv. Mater.* **2009**, *21*, 139–152.
7. White, C. T.; Todorov, T. N. Quantum Electronics−Nanotubes Go Ballistic. *Nature* **2001**, *411*, 649–651.
8. Zhou, O.; Shimoda, H.; Gao, B.; Oh, S.; Fleming, L.; Yue, G. Materials Science of Carbon Nanotubes: Fabrication, Integration, and Properties of Macroscopic Structures of Carbon Nanotubes. *Acc. Chem. Res.* **2002**, *35*, 1045–1053.
9. Ajayan, P. M.; Tour, J. M. Materials Science−Nanotube Composites. *Nature* **2007**, *447*, 1066–1068.
10. Singh, P.; Campidelli, S.; Giordani, S.; Bonifazi, D.; Bianco, A.; Prato, M. Organic Functionalization and Characterization of Single-Walled Carbon Nanotubes. *Chem. Soc. Rev.* **2009**, *38*, 2214–2230.
11. Tasis, D.; Tagmatarchis, N.; Bianco, A.; Prato, M. Chemistry of Carbon Nanotubes. *Chem. Rev.* **2006**, *106*, 1105–1136.
12. Peng, X.; Wong, S. S. Functional Covalent Chemistry of Carbon Nanotube Surfaces. *Adv. Mater.* **2009**, *21*, 625–642.
13. Huang, W.; Fernando, K. A. S.; Allard, L. F.; Sun, Y. P. Solubilization of Single-Walled Carbon Nanotubes with Diamine-Terminated Oligomeric Poly(ethylene glycol) in Different Functionalization Reactions. *Nano Lett.* **2003**, *3*, 565–568.
14. Zhou, B.; Lin, Y.; Li, H.; Huang, W.; Connell, J. W.; Allard, L. F.; Sun, Y. P. Absorptivity of Functionalized Single-Walled Carbon Nanotubes in Solution. *J. Phys. Chem. B* **2003**, *107*, 13588–13592.
15. Georgakilas, V.; Kordatos, K.; Prato, M.; Guldi, D. M.; Holzinger, M.; Hirsch, A. Organic Functionalization of Carbon Nanotubes. *J. Am. Chem. Soc.* **2002**, *124*, 760–761.
16. Tagmatarchis, N.; Prato, M. Functionalization of Carbon Nanotubes *via* 1,3-Dipolar Cycloadditions. *J. Mater. Chem.* **2004**, *14*, 437–439.
17. Zhao, B.; Hu, H.; Yu, A. P.; Perea, D.; Haddon, R. C. Synthesis and Characterization of Water Soluble Single-Walled Carbon Nanotube Graft Copolymers. *J. Am. Chem. Soc.* **2005**, *127*, 8197–8203.
18. Kam, N. W. S.; O'Connell, M.; Wisdom, J. A.; Dai, H. Carbon Nanotubes as Multifunctional Biological Transporters and Near-Infrared Agents for Selective Cancer Cell Destruction. *Proc. Natl. Acad. Sci. U.S.A.* **2005**, *102*, 11600–11605.
19. Nakayama-Ratchford, N.; Bangsaruntip, S.; Sun, X.; Welsher, K.; Dai, H. Noncovalent Functionalization of Carbon Nanotubes by Fluorescein-Polyethylene glycol: Supramolecular Conjugates with pH-Dependent Absorbance and Fluorescence. *J. Am. Chem. Soc.* **2007**, *129*, 2448–2449.
20. Lin, Y.; Taylor, S.; Li, H. P.; Fernando, K. A. S.; Qu, L. W.; Wang, W.; Gu, L. R.; Zhou, B.; Sun, Y. P. Advances Toward Bioapplications of Carbon Nanotubes. *J. Mater. Chem.* **2004**, *14*, 527–541.
21. Kitaygorodskiy, A.; Wang, W.; Xie, S. Y.; Lin, Y.; Fernando, K. A. S.; Wang, X.; Qu, L. W.; Chen, B.; Sun, Y. P. NMR Detection of Single-Walled Carbon Nanotubes in Solution. *J. Am. Chem. Soc.* **2005**, *127*, 7517–7520.
22. Blighe, F. M.; Blau, W. J.; Coleman, J. N. Towards Tough, yet Stiff, Composites by Filling an Elastomer with Single-Walled Nanotubes at Very High Loading Levels. *Nanotechnology* **2008**, *19*, 415709–415715.
23. Singh, R.; Pantarotto, D.; Lacerda, L.; Pastorin, G.; Klumpp, C.; Prato, M.; Bianco, A.; Kostarelos, K. Tissue Biodistribution and Blood Clearance Rates of Intravenously Administered Carbon Nanotube Radiotracers. *Proc. Natl. Acad. Sci. U.S.A.* **2006**, *103*, 3357–3362.
24. Liu, Z.; Cai, W.; He, L.; Nakayama, N.; Chen, K.; Sun, X. G.; Chen, X.; Dai, H. *In Vivo* Biodistribution and Highly Efficient Tumour Targeting of Carbon Nanotubes in Mice. *Nat. Nanotechnol.* **2007**, *2*, 47–52.
25. Dumortier, H.; Lacotte, S.; Pastorin, G.; Marega, R.; Wu, W.; Bonifazi, D.; Briand, J. P.; Prato, M.; Muller, S.; Bianco, A. Functionalized Carbon Nanotubes are Non-cytotoxic and Preserve the Functionality of Primary Immune Cells. *Nano Lett.* **2006**, *6*, 1522–1528.
26. Yang, S. T.; Fernando, K. A. S.; Liu, J. H.; Wang, J.; Sun, H. F.; Liu, Y.; Chen, M.; Huang, Y.; Wang, X.; Wang, F.; *et al.* Covalently PEGylated Carbon Nanotubes with Stealth Character *in Vivo*. *Small* **2008**, *4*, 940–944.
27. Van Vlerken, L. E.; Vyas, T. K.; Amiji, M. M. Poly(ethylene glycol)-Modified Nanocarriers for Tumor-Targeted and Intracellular Delivery. *Pharm. Res.* **2007**, *24*, 1405–1414.
28. Bekyarova, E.; Ni, Y.; Malarkey, E. B.; Montana, V.; McWilliams, J. L.; Haddon, R. C.; Parpura, V. Applications of Carbon Nanotubes in Biotechnology and Biomedicine. *J. Biomed. Nanotechnol.* **2005**, *1*, 3–17.
29. Zanello, L. P.; Zhao, B.; Hu, H.; Haddon, R. C. Bone Cell Proliferation on Carbon Nanotubes. *Nano Lett.* **2006**, *6*, 562–567.
30. Cellot, G.; Cilia, E.; Cipollone, S.; Rancic, V.; Sucapane, A.; Giordani, S.; Gambazzi, L.; Markram, H.; Grandolfo, M.; Scaini, D.; et al. Carbon Nanotubes Might Improve Neuronal Performance by Favouring Electrical Shortcuts. *Nat. Nanotechnol.* **2008**, *4*, 126–133.
31. Lovat, V.; Pantarotto, D.; Lagostena, L.; Cacciari, B.; Grandolfo, M.; Righi, M.; Spalluto, G.; Prato, M.; Ballerini, L. Carbon Nanotube Substrates Boost Neuronal Electrical Signaling. *Nano Lett.* **2005**, *5*, 1107–1110.
32. Morris, K. F.; Johnson, C. S. Diffusion-Ordered 2-Dimensional Nuclear-Magnetic-Resonance Spectroscopy. *J. Am. Chem. Soc.* **1992**, *112*, 3139–3141.
33. Gounarides, J. S.; Chen, A.; Shapiro, M. J. Nuclear Magnetic Resonance Chromatography: Applications of Pulse Field Gradient Diffusion NMR to Mixture Analysis and Ligand-Receptor Interactions. *J. Chromatogr. B* **1999**, *725*, 79–90.
34. Kellenbach, E.; Burgering, M.; Kaspersen, F. Using Pulse Field Gradient NMR-Based Diffusion Experiments to Identify Signals of Low-Molecular-Weight Impurities. *Org. Process Res. Dev.* **1999**, *3*, 141–144.
35. Cohen, Y.; Avram, L.; Frish, L. Diffusion NMR Spectroscopy in Supramolecular and Combinatorial Chemistry: An Old

Parameter—New Insights. *Angew. Chem., Int. Ed.* **2005**, *44*, 520–544.
36. Kapur, G. S.; Cabrita, E. J.; Berger, S. The Qualitative Probing of Hydrogen Bond Strength by Diffusion-Ordered NMR Spectroscopy. *Tetrahedron Lett.* **2000**, *41*, 7181–7185.
37. Viel, S.; Mannina, L.; Segre, A. Detection of a $\pi-\pi$ Complex by Diffusion-Ordered Spectroscopy (DOSY). *Tetrahedron Lett.* **2002**, *43*, 2515–2519.
38. Rudzevich, Y.; Rudzevich, V.; Moon, C.; Brunklaus, G.; Böhmer, V. Self-Assembled Dendrimers with Uniform Structure. *Org. Biomol. Chem.* **2008**, *6*, 2270–2275.
39. Santos, J. I.; de Souza, A. C.; Cañada, F. J.; Martín-Santamaría, S.; Kamerling, J. P.; Jiménez-Barbero, J. Assessing Carbohydrate−Carbohydrate Interactions by NMR Spectroscopy: The Trisaccharide Epitope from the Marine Sponge Microciona Prolifera. *ChemBioChem* **2009**, *10*, 511–519.
40. Viel, S.; Capitani, D.; Mannina, L.; Segre, A. Diffusion-Ordered NMR Spectroscopy: A Versatile Tool for the Molecular Weight Determination of Uncharged Polysaccharides. *Biomacromolecules* **2003**, *4*, 1843–1847.
41. Morris, K. F.; Johnson Jr, C. S. Resolution of Discrete and Continuous Molecular Size Distributions by Means of Diffusion-Ordered 2D NMR Spectroscopy. *J. Am. Chem. Soc.* **1993**, *115*, 4291–4299.
42. Sorbi, C.; Bergamin, M.; Bosi, S.; Dinon, F.; Aroulmoji, V.; Khan, R.; Murano, E.; Norbedo, S. Synthesis of 6-*O*-Methotrexylhyaluronan as a Drug Delivery System. *Carbohydr. Res.* **2009**, *344*, 91–97.
43. Durand, J.; Fernández, F.; Barrière, C.; Teuma, E.; Gómez, K.; González, G.; Gómez, M. DOSY Technique Applied to Palladium Nanoparticles in Ionic Liquids. *Magn. Reson. Chem.* **2008**, *46*, 739–743.
44. Evangelisti, C.; Raffa, P.; Balzano, F.; Barretta, G. U.; Vitulli, G.; Salvadori, P. Size-Controlled Synthesis and NMR Characterization of Mesitylene−Vinylsiloxanes-Stabilized Pt Nanoparticles in Solution. *J. Nanosci. Nanotechnol.* **2008**, *8*, 2096–2101.
45. Fielden, J.; Long, D. L.; Slawin, A. M. Z.; Kögerler, P.; Cronin, L. Ligand and Counterion Control of Ag(I) Architectures: Assembly of a {Ag-8} Ring Cluster Mediated by Hydrophobic and Ag···Ag Interactions. *Inorg. Chem.* **2007**, *46*, 9090–9097.
46. Van Lokeren, L.; Maheut, G.; Ribot, F.; Escax, V.; Verbruggen, I.; Sanchez, C.; Martins, J. C.; Biesemans, M.; Willem, R. Characterization of Titanium Dioxide Nanoparticles Dispersed in Organic Ligand Solutions by Using a Diffusion-Ordered Spectroscopy-Based Strategy. *Chem.—Eur. J.* **2007**, *13*, 6957–6966.
47. Gabriel, C. J.; DeMatteo, M. P.; Paul, N. M.; Takaya, T.; Gustafson, T. L.; Hadad, C. M.; Parquette, J. R. A New Class of Intramolecularly Hydrogen-Bonded Dendrons Based on a 2-Methoxyisophthalamide Repeat Unit. *J. Org. Chem.* **2006**, *71*, 9035–9044.
48. Klumpp, C.; Lacerda, L.; Chaloin, O.; Da Ros, T.; Kostarelos, K.; Prato, M.; Bianco, A. Multifunctionalised Cationic Fullerene Adducts for Gene Transfer: Design, Synthesis and DNA Complexation. *Chem. Commun.* **2007**, 3762–3764.
49. Kato, H.; Böttcher, C.; Hirsch, A. Sugar Balls: Synthesis and Supramolecular Assembly of [60]Fullerene Glycoconjugates. *Eur. J. Org. Chem.* **2007**, *16*, 2659–2666.
50. Marega, R.; Aroulmoji, V.; Dinon, F.; Vaccari, L.; Giordani, S.; Bianco, A.; Murano, E.; Prato, M. Diffusion-Ordered NMR Spectroscopy in the Structural Characterization of Functionalized Carbon Nanotubes. *J. Am. Chem. Soc.* **2009**, *131*, 9086–9093.
51. Loening, M. N.; Keeler, J.; Morris, G. A. One-Dimensional DOSY. *J. Magn. Reson.* **2001**, *153*, 103–112.
52. Bonifazi, D.; Nacci, C.; Marega, R.; Campidelli, S.; Ceballos, G.; Modesti, S.; Meneghetti, M.; Prato, M. Microscopic and Spectroscopic Characterization of Paintbrush-Like Single-Walled Carbon Nanotubes. *Nano Lett.* **2006**, *6*, 1408–1414.
53. Stejskal, E. O.; Tanner, J. E. Spin Diffusion Measurements: Spin Echoes in the Presence of a Time-Dependent Field Gradient. *J. Chem. Phys.* **1965**, *42*, 288–292.
54. Ebersold, M. F.; Zydney, A. L. Separation of Protein Charge Variants by Ultrafiltration. *Biotechnol. Prog.* **2004**, *20*, 543–549.
55. Lajmi, A. R.; Schwartz, L.; Sanghvi, Y. S. Membrane Purification of an Antisense Oligonucleotide. *Org. Process Res. Dev.* **2004**, *8*, 651–657.
56. Limayem, I.; Charcosset, C.; Fessi, H. Purification of Nanoparticle Suspensions by a Concentration/Diafiltration Process. *Sep. Purif. Technol.* **2004**, *38*, 1–9.
57. Rinzler, A. G.; Liu, J.; Dai, H.; Nikolaev, P.; Huffman, C. B.; Rodriguez-Macias, F. J.; Boul, P. J.; Lu, A. H.; Heymann, D.; Colbert, D. T. Large-Scale Purification of Single-Wall Carbon Nanotubes: Process, Product, and Characterization. *Appl. Phys. A: Mater. Sci. Process.* **1998**, *67*, 29–37.
58. Sweeney, S. F.; Woehrle, G. H.; Hutchison, J. E. Rapid Purification and Size Separation of Gold Nanoparticles *via* Diafiltration. *J. Am. Chem. Soc.* **2006**, *128*, 3190–3197.
59. Sun, Y. P.; Fu, K.; Lin, Y.; Huang, W. Functionalized Carbon Nanotubes: Properties and Applications. *Acc. Chem. Res.* **2002**, *35*, 1096–1104.
60. Huanny, W.; Fernando, S.; Lin, Y.; Zhou, B.; Allard, L. F.; Sun, Y. P. Preferential Solubilization of Smaller Single-Walled Carbon Nanotubes in Sequential Functionalization Reactions. *Langmuir* **2003**, *19*, 7084–7088.
61. Sun, Y. P.; Huang, W.; Lin, Y.; Fu, K.; Kitaygorodskiy, A.; Riddle, L. A.; Yu, Y. J.; Carroll, D. L. Soluble Dendron-Functionalized Carbon Nanotubes: Preparation, Characterization, and Properties. *Chem. Mater.* **2001**, *13*, 2864–2869.
62. Delsuc, M. A.; Malliavin, T. E. Maximum Entropy Processing of DOSY NMR Spectra. *Anal. Chem.* **1998**, *70*, 2146–2148.
63. Herrero, M. A.; Toma, F. M.; Al-Jamal, K. T.; Kostarelos, K.; Bianco, A.; Da Ros, T.; Bano, F.; Casalis, L.; Scoles, G.; Prato, M. Synthesis and Characterization of a Carbon Nanotube−Dendron Series for Efficient siRNA Delivery. *J. Am. Chem. Soc.* **2009**, *131*, 9843–9848.